

Performance of different tungsten grades under transient thermal loads

J. Linke 1), T. Loewenhoff 1), V. Massaut 2), G. Pintsuk 1), G. Ritz 1), M. Rödiger 1), A. Schmidt 1), C. Thomser 1), I. Uytendhouwen 2), V. Vasechko 1), M. Wirtz 1)

1) Forschungszentrum Jülich GmbH, EURATOM Association, D-52425 Jülich, Germany

2) SCK•CEN, The Belgian Nuclear Research Centre, Association EURATOM, 2400 Mol, Belgium

e-mail contact main author: j.linke@fz-juelich.de

Abstract. Plasma facing components in future thermonuclear fusion devices will be subjected to intense transient thermal loads due to Edge Localized Modes (type I ELMs), plasma disruptions etc.. To exclude irreversible damage to the divertor targets, local energy deposition must remain below the damage threshold for the selected wall materials. For monolithic tungsten (pure tungsten and tungsten alloys) power densities above $\approx 0.3 \text{ GW/m}^2$ with 1 ms duration result in the formation of a dense crack network. Thin tungsten coatings for the so-called ITER-like wall in JET, which have been deposited on a 2-directional carbon-fiber composite (CFC) material, are even less resistant to thermal shock damage; here the threshold values are by a factor of 2 lower. First ELM-simulation experiments with high cycle numbers up to 10^4 cycles on actively cooled bulk tungsten targets do not reveal any cracks for absorbed power densities up to 0.2 GW/m^2 and ELM-durations in the sub-millisecond range (0.8 ms); at somewhat higher power densities (0.27 GW/m^2 , $\Delta t = 0.5 \text{ ms}$) cracks have been detected for 10^6 cycles.

1. Introduction

The thermal loads to the divertor and the first wall in next step magnetic confinement experiments such as ITER will originate from two stimulating factors. These are quasi-stationary heat fluxes with power densities up to about 10 MW/m^2 and very short transients, which occur during plasma instabilities in the boundary layer (Edge Localized Modes or type I ELMs) with power densities up to the GW/m^2 -range [1]. While thermal equilibrium will be achieved rather rapidly during steady-state loads, the transient ELM loads will interfere with the plasma facing wall only for very short periods in the sub-millisecond range. However, these events occur with high frequencies of about 1 Hz or higher, thus accumulating millions of events during the lifetime of the component. To investigate the performance of bulk tungsten, W-alloys and thin W-coatings under intense transients small test coupons cut from these materials were exposed to 1 ms beam pulses in an electron beam test facility. In general, these tests were carried out with 100 repeated pulses in a wide temperature range which represents the operation conditions in ITER. To gain additional information on the performance of these materials under repetitive loads with very high cycle numbers, additional tests were conducted with enhanced repetition rates (e.g. $f = 25 \text{ Hz}$) on tungsten-armoured actively cooled components.

The thermal shock induced crack pattern depends strongly on the microstructure (grain shape and size) of the used tungsten grade; in addition, alloying elements can have significant impact on the response to intense transient loads and on the mechanical stability. To quantify these effects a number of tungsten grades, which have undergone different deformation processes, alloyed tungsten and tungsten coatings have been investigated in comprehensive electron beam studies. A detailed materials characterization programme including laser profilometry, optical and scanning electron microscopy, and metallography has been applied to all test coupons and components. To provide an almost complete set of material data including physical and mechanical characteristics, further detailed analyses have been performed in close collaboration between Forschungszentrum Jülich (FZJ) and the Belgian nuclear research center in Mol (SCK•CEN) [2].

2. Materials

The transient heat load tests have been performed on a number of different tungsten grades with different purity and deformation processes. Beside standard grades with a purity of 99.97 weight% also ultra high purity tungsten (W-UHP, 99.9999 weight%) has been investigated. In addition alloys with 1 and 5 weight% tantalum (W-Ta1, W-Ta5) and a potassium doped grade (WVMW, 15 – 40 ppm K) were investigated. These materials have undergone different densification processes: forging of sintered W into cylindrical shape results in elongated grain texture parallel to the cylinder axis. Another deformation process, namely hot forging of sintered W-cylinders into round blanks results in flattened grains parallel to the front face. A so-called ‘double forging’ treatment, i.e. a combination of the two above mentioned deformation processes has been applied to a pure tungsten material; the sequential application of these two manufacturing routes reduces the anisotropy in the material, which is generally applied by the deformation processes. All bulk materials in this study have been provided by Plansee AG, Austria.

Tungsten coatings with a thickness of about 25 μm were produced by a Combined Magnetron Sputtering and Ion Implantation (CMSII) coating technique at the INFLPR, Romania [3]. The substrate consists of a 2-directional carbon-fibre composite material (DMS 780, Dunlop, UK) with one of the fibre planes being oriented perpendicular and one parallel to the coated surface. To improve the adhesion between tungsten and carbon a thin molybdenum interlayer has been intercalated.

3. Simulation of ITER relevant transient thermal loads

To simulate ELM-specific thermal loads in the sub-millisecond range with ITER relevant energy densities plasma accelerators or electron beam test facilities are used. Quasi Stationary Plasma Accelerators (QSPA) are suited best to emulate the plasma wall interaction during ELMs [4, 5]; however, this test equipment is less qualified to perform repetitive tests with high cycle or large specimen numbers. Here the electron beam test beds outmatch the QSPA facilities. All experiments described in this paper were performed in the two high power electron beam test facilities JUDITH 1 and 2 at FZJ [6]. In these experiments tests coupons of typically $12 \times 12 \times 5 \text{ mm}^3$ were used. In the case of bulk tungsten the electron beam exposed surfaces were oriented perpendicular to the axis of the forged rods or to the forging direction in the case of the hot-forged blanks. All surfaces of the non-coated test coupons were polished to remove pre-existing surface damages originating for the spark-erosion machining and to allow a precise detection of thermal shock induced roughening or surface cracks.

The test coupons were mounted on a heated sample holder; the experiments were done in a temperature range from RT up to 600°C . In JUDITH 1 a homogenous heat load distribution in the $4 \times 4 \text{ mm}^2$ beam spot was achieved by a triangular scanning of the 1 mm wide Gaussian shaped electron beam (31 / 40 kHz). The pulse duration was fixed to 1 ms with an inter pulse time of 2 s. All experiments described in this paper were performed with 100 identical beam pulses. In separate experiments the absorbed power density was varied stepwise up to 1.3 GW/m^2 for the bulk W test coupons, and up to 0.3 GW/m^2 for the W-coatings. In-situ diagnostics, which were applied during the transient heat load tests, were a fast single-colour pyrometer (500 ... 2500°C), an IR camera system (RT ... 2000°C), and CCD cameras for optical observation, e.g. of particle erosion. All experiments with high repetition rates ($10^3 - 10^6$ pulses) were performed on actively cooled tungsten tiles brazed to a water cooled copper holder; these tests were performed in JUDITH 2; details on the beam scanning mode are described below.

Typical results from ELM simulation experiments with 100 identical beam pulses are listed in FIG. 1 for UHP tungsten. For heat loads below the damage threshold, e.g. for 0.16 GW/m^2 for a surface temperature of 400°C , the polished tungsten surface does not show any modification. If the heat load is increased (e.g. to 0.63 GW/m^2), irreversible damage of the tungsten surface has been observed. As long as the temperature of the test coupon is high enough to deform plastically, the electron beam exposed surface shows a clear roughening, but the formation of cracks is suppressed. A dense crack network is formed when the test coupon is exposed to the same thermal load at room temperature (RT). Here the crack pattern consists of two crack types, primary cracks with a long depth range of about $500 \mu\text{m}$ and deeper, and secondary cracks which in general extend only to a few ten microns, i.e. to a depth which is determined by the penetration of the heat front during the ELM event and the associated thermal stress due to expansion of the material.

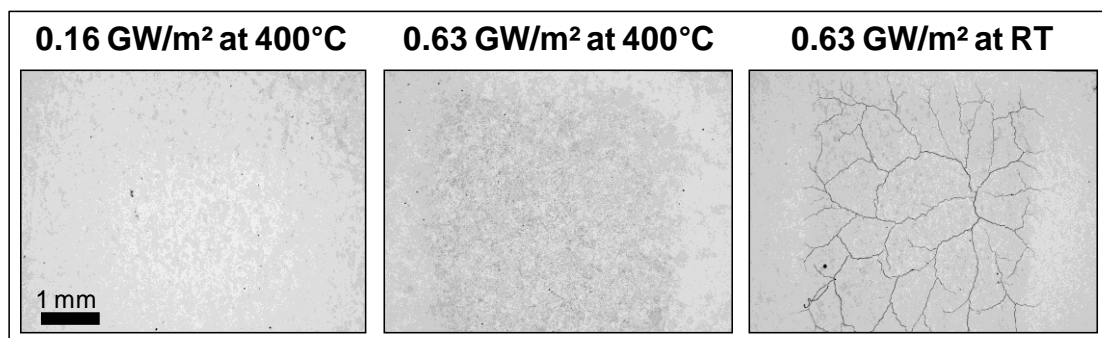


FIG. 1: Material damage on sintered UHP tungsten at different thermal loads P_{abs} and base temperatures (100 electron beam pulses, $\Delta t = 1 \text{ ms}$, $P_{abs} / P_{inc} = 0.46$)
left: no visible degradation, centre: surface roughening, right: intense crack network)

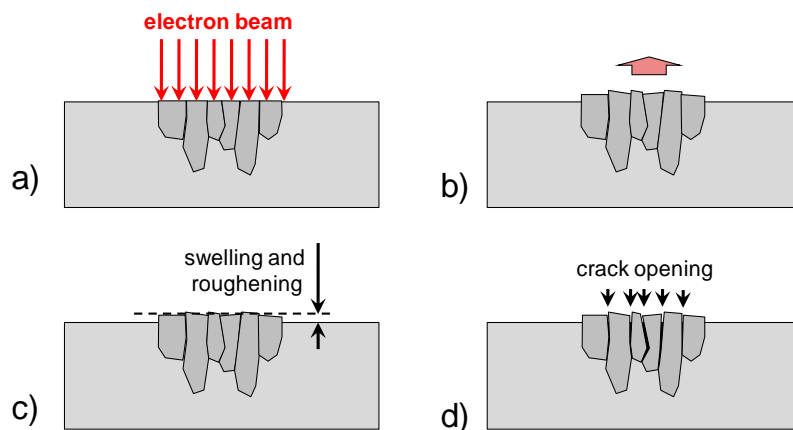


FIG. 2: Schematic presentation of the response of tungsten with anisotropic grain texture to short transient loads using focussed electron beams.

This roughening and crack formation process during electron beam is shown schematically in FIG. 2. The incident electron beam pulse will only affect a shallow surface layer; the depth of this zone is determined on the one hand by the penetration depth of the 120 keV electrons, which is only in a range from 5 to $10 \mu\text{m}$, on the other hand by the penetration depth of the heat wave during the 1 ms pulse, which is approximately one order of magnitude larger. Due to the extreme heat flux, the temperature increase in this thin layer will be several hundred K, thereby crossing the material's Ductile to Brittle Transition Temperature (DBTT); this fact facilitates the thermal expansion and the irreversible, plastic deformation of the heated grains due to compressive stresses during loading (FIG. 2b). As a consequence, after the cool down

an irreversible swelling (up to a few microns) and a roughening of the surface can be detected (FIG. 2c). Since the subjacent tungsten remains thermally unaffected, the cool down will occur rapidly, thus preventing any stress relief at high temperature. This may result in crack formation due to the volumetric shrinkage and the correlated high tensile stresses preferably at the weak grain boundaries when returning to its brittle state. (FIG. 2d).

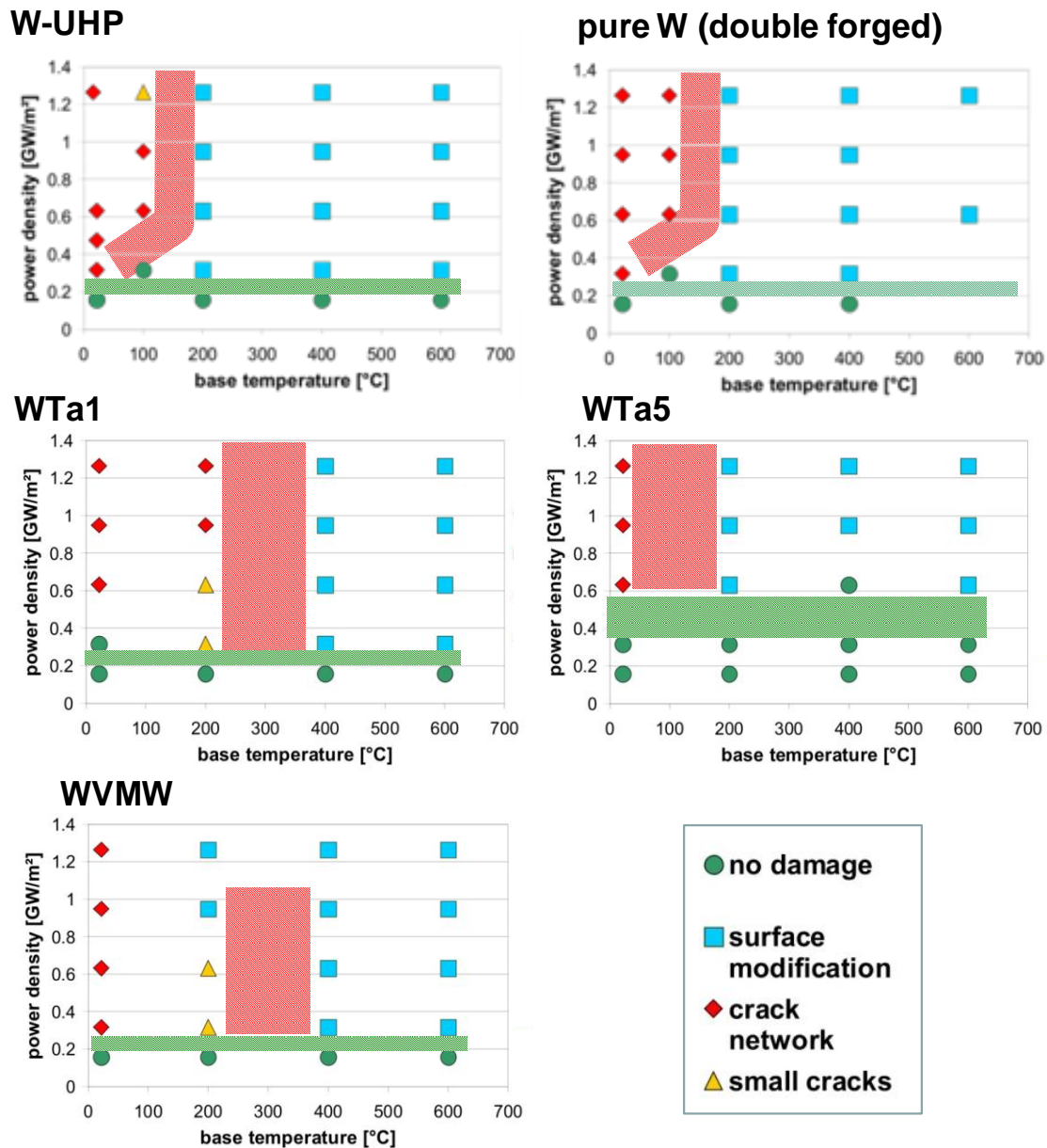


FIG. 3: Thermally induced surface modifications in different tungsten grades after repeated electron beam pulses of 1 ms duration. For each data point 100 electron beam pulses have been applied at different temperatures and at different base temperatures of the test coupons.

The loading parameters at which these two above mentioned processes (roughening and crack formation) become essential, strongly depend on the microstructure and the thermo-mechanical properties of the materials. Therefore, alloying of the bulk tungsten has a significant impact on the threshold values for surface roughening and crack formation as shown in FIG. 3. In this figure the ELM-induced response of the 5 different tungsten grades has been analyzed for different incident power densities and different base temperatures of the

test coupons during electron beam heating. Both undoped grades, W-UHP and pure double forged tungsten, show a rather similar behaviour: the threshold heat flux for roughening (green bar) is clearly below 0.3 GW/m^2 , while the cracking threshold (red bar) is mainly determined by the ductile to brittle transition and was found to be in a range between 100 and 200°C . Tungsten alloys with relatively low concentrations of the alloying elements such as WTa1 or WVMW show the same roughening threshold, but a much higher cracking threshold (between 200 and 400°C). Significant improvements of the material performance under transient thermal loads have only been found for the tungsten alloy WTa5 with 5% of tantalum. Here roughening effects have only been detected for power densities clearly above 0.4 GW/m^2 . It should be noted that due to the anisotropic texture of these materials the crack initiation and crack growth is strongly affected by the grain shape and the grain orientation with respect to the heat flux direction [7]. Hence, cracks with an orientation parallel to the heated surface and subsequent delamination effects can be the main reason for an overheating, melting and complete loss of the detached layer.

Similar ELM-simulation tests have been applied to the tungsten coatings on the CFC substrates. In these experiments the power densities on the loaded surface of $4 \times 4 \text{ mm}^2$ were limited to 0.32 GW/m^2 and the surface temperature was kept between RT and 400°C . The overall performance of the coated CFC tile is shown in FIG. 4 in analogy to the bulk tungsten tests in FIG. 3. First surface modifications were detected for power densities of about 0.1 GW/m^2 . Since the surface of the coating has not been polished, roughening effects are difficult to detect. The observed surface modifications mainly represent changes in the reflectivity induced by the incident electron beam. First cracks and/or delamination of the coatings were detected after 100 beam pulses with a surface heat load of 0.16 GW/m^2 ; above 0.24 GW/m^2 a major fraction of the coating was severely damaged due to delamination, cracking, and melting.

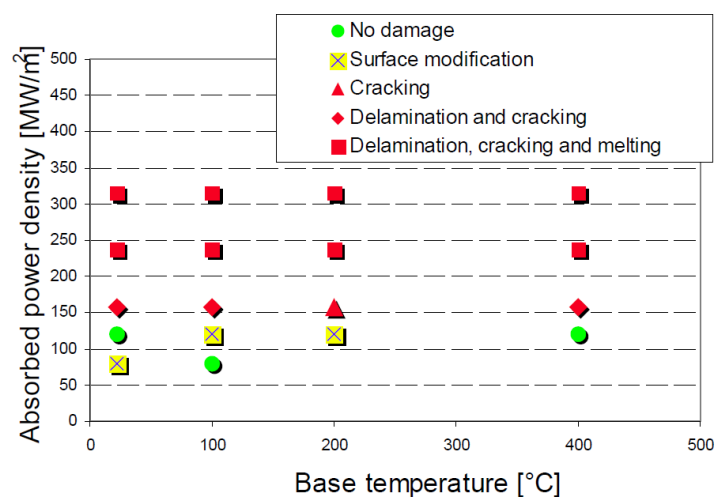


FIG. 4: Damage threshold for thin tungsten coatings on CFC substrates after electron beam exposure to 100 pulses of 1 ms duration.

To avoid an overheating of the tungsten coating during steady state plasma exposure and during transients in JET [8], the carbon fibres within the CFC tile were oriented as shown schematically in FIG. 5. This configuration allows excellent heat removal by the fibres which are aligned perpendicular to the surface (i.e. parallel to the incident heat flux) and moderate thermal conductivity for the felt layer. Fibres which are aligned parallel to the surface can

only contribute insignificantly to the heat removal. In addition, these fibres show the largest mismatch in CTE if compared with the parameters of the W-Mo coating.

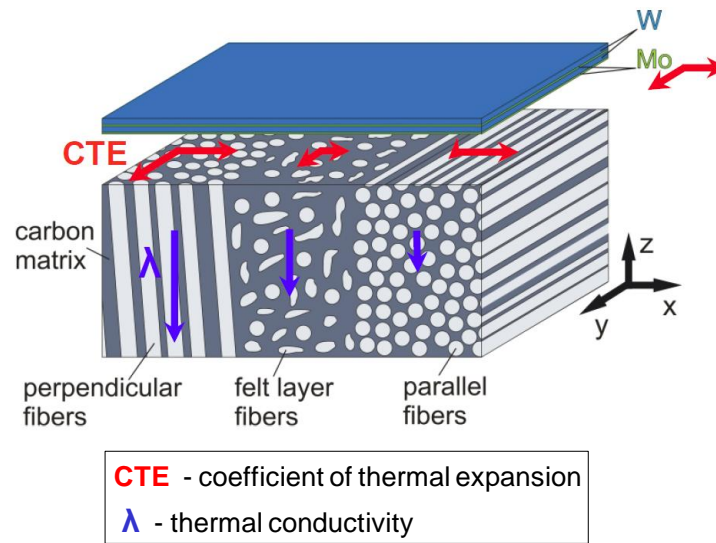


FIG. 5: Schematic presentation of the magnetron sputtered double layer coating on the carbon fibre composite substrate (DMS 780). The CFC consists of three different regions: fibres which are oriented perpendicularly to the surface (left), parallel fibres (right) and a felt layer with randomly oriented short fibres in between. The length of the blue and red arrows indicate the thermal conductivity of the three regions and the CTE values in the interface region, respectively.

		Base temperature, °C			
		RT	100	200	400
APD, MW/m ²	316	par. felt per.	par. felt per.	par. felt per.	par. felt per.
	237	par. felt per.	par. felt per.	par. felt per.	par. felt per.
	158	par. felt per.	par. felt per.	par. felt per.	par. felt per.
	121	par. felt per.	par. felt per.	par. felt per.	par. felt per.
	79	par. felt per.	par. felt per.	par. felt per.	par. felt per.

TABLE 1: Thermal response of thin W coatings on DMS 780. APD - absorbed power density; par. - parallel oriented fibres, felt - felt layer, per. - perpendicular oriented fibres
green - no damage; orange - moderate damage; red - heavy damage.

This geometry has significant impact on the high heat flux performance of the coated tile. Regions with perpendicularly aligned fibres show the best CTE match; in addition, the heat removal is best due to the relatively high thermal conductivity of the fibres. On the other hand, fibres oriented parallel to the surface show the worst CTE mismatch and the least thermal conductivity. Therefore, delamination of the coating and overheating due to the detachment is expected to occur first on the parallel fibres. In addition, the poor thermal conductivity of this region will amplify this deterioration effect.

A detailed analysis of the thermal shock induced damage of the W-coating is shown in TABLE 1. The colour code in this table makes clear that the performance of the coating depends essentially on the texture of the substrate. The 25 μm coating can withstand severe

transients of 1 ms duration of more than 0.2 GW/m^2 . This threshold value is in good agreement with the data which were derived for the pure tungsten grades or to those with low concentrations of the alloying elements. In contrast, coatings on the parallel fibres fail much earlier and can only be subjected to mitigated ELMs with 0.12 GW/m^2 or slightly above. It also should be noted that the thermal response of the tungsten coatings shows no clear temperature dependence; obviously the substrate plays a dominant role during thermal shock loading [9].

To study the behaviour of plasma facing materials under very large cycle numbers (10^6 events or higher) which are expected during the lifetime of the ITER divertor a new experimental procedure is required which allows an accelerated loading scheme with individual pulses with ITER relevant power densities and pulse durations. This can only be achieved on actively cooled test samples which allow to remove the excess heat from the test coupons. In addition it must be guaranteed that the surface temperature of the test coupons remains in a fusion specific range of several hundred degree C throughout the experiment. All these boundary conditions can only be fulfilled in a high power test device with sufficient flexibility of the beam guidance such as the 200 kW electron beam test device JUDITH 2 [10, 11] at FZJ.

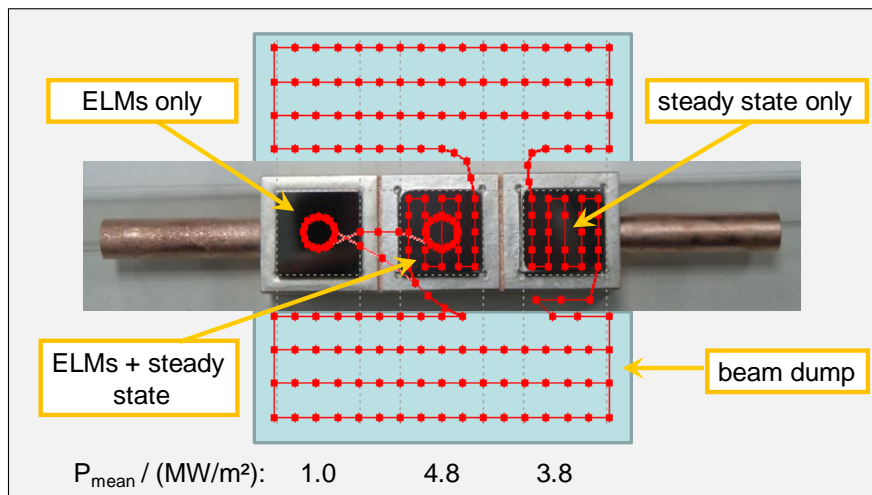


FIG. 6: Electron beam path during ELM-simulation experiments on an actively cooled tungsten module (beam diameter: 6 mm, $P_{ELM} \geq 200 \text{ MW/m}^2$, repetition rate: 25 Hz)

The principle of the experimental procedure is shown in FIG. 6. Due to the high flexibility of the beam positioning system it can be used to apply ELM-like loads of 500 μs duration by a circular beam motion (left tile; dwell time on each beam spot is 5 μs). In between two ELM events the beam can be diverted to a beam dump (blue area) or it can be used to simulate steady state heat loads on individual test coupons (right tile). The ideal configuration can be obtained by the superposition of both states (central tile); under these conditions a mean quasi-stationary heat load $P_{\text{mean}} = 4.8 \text{ MW/m}^2$ can be achieved, which will guarantee a tile surface temperature of 400 – 800°C depending on the geometry of the heat sink, the tile thickness, and the coolant flow rate.

First experiments using the above mentioned testing procedure for an ELM-duration of 0.8 ms and an absorbed power density of 0.2 GW/m^2 do not reveal any surface modifications for 10^3 cycles and roughening after 10^4 cycles. An increase of the ELM power density to 0.37 GW/m^2 at 0.5 ms clearly reconfirms the threshold values obtained on the un-cooled test specimens also for medium cycle numbers ($n = 10^4$). In one particular experiment 10^6 ELM-specific thermal shocks ($P_{\text{abs}} = 0.27 \text{ GW/m}^2$, $\Delta t = 0.5 \text{ ms}$) have been applied to a water cooled

target with pure tungsten tiles which have been attached by high-temperature brazing. Under these conditions clear roughening and crack formation have been observed. The microstructural characteristics of the electron beam loaded tungsten surface are shown in FIG. 7.

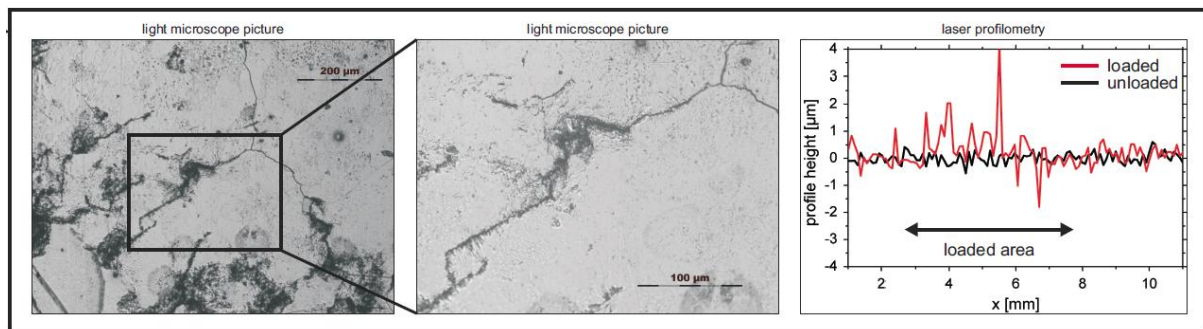


FIG. 7: Pure tungsten after 10^6 simulated ELM events ($P_{abs} = 0.27 \text{ GW/m}^2$, $\Delta t = 0.5 \text{ ms}$) which have been applied in the electron beam test facility JUDITH 2.

4. Conclusion

The thermal response to intense electron beam pulses depends strongly on the texture of the bulk tungsten grade and in the case of W-coatings on the texture of the underlying CFC substrate. Pure tungsten grades or alloys with low concentrations of the alloying elements in general do not show any damage for power densities of $P_{abs} = 0.16 \text{ GW/m}^2$ at $\Delta t = 1 \text{ ms}$ pulse duration for 100 pulses. These data correspond to a heat flux factor $f_{HF} = P_{abs} \Delta t^{0.5} = 5.1 \text{ MWm}^{-2}\text{s}^{0.5}$. Alloys with 5 % tantalum show a better performance; here a heat flux factor $f_{HF} = 10.1 \text{ MWm}^{-2}\text{s}^{0.5}$ did not result in any material cracking or modification. For the tungsten coatings on the CFC substrate the damage threshold was lower; this material could be exposed to intense electron beam pulses up to $f_{HF} 3.8 \text{ MWm}^{-2}\text{s}^{0.5}$. However, on limited areas where the fibres were oriented parallel to the incident heat flux the f_{HF} at the damage threshold could be doubled. First experiments with high cycle numbers in JUDITH 2 show undamaged tungsten surfaces up to $f_{HF} 5.7 \text{ MWm}^{-2}\text{s}^{0.5}$ for 10^3 but roughening after 10^4 cycles. A slight increase of the f_{HF} to $6.0 \text{ MWm}^{-2}\text{s}^{0.5}$ results in surface roughening and crack formation after exposure to 10^6 ELM events.

5. References

- [1] A. Loarte et al., this conference
- [2] G. Pintsuk, I. Uytendhouwen, Int. Journal of Refractory Metals and Hard Materials, in press
- [3] C. Ruset et al., Fusion Engineering and Design 84, 2009, 1662
- [4] N. Klimov et al., J. Nucl. Mater. 390 – 391, 2009, 721 - 726
- [5] K. Wittlich et al, Fusion Engineering and Design, 84, 2009, 1982-1986
- [6] G. Pintsuk et al., Proc. ICFRM-14, Sapporo, 7-12, September, 2009
- [7] M. Wirtz et al., Proc. Annual Meeting on Nuclear Technology, Berlin, 04.–06.05.2010
- [8] G.F. Matthews et al., Physica Scripta T138, 2009, 014030
- [9] C. Thomser et al., Proc. Int. Conf. and School on Plasma Physics and Controlled Fusion Alushta, Ukraine, 13. - 18.09. 2010
- [10] Th. Loewenhoff, A. Bürger, J. Linke, G. Pintsuk, A. Schmidt, Proc. 26th Symposium on Fusion Technology, Porto, Portugal, 27.09. – 01.10.2010
- [11] Th. Loewenhoff et al., Proc. Annual Meeting on Nuclear Technology, Berlin, 04.–06.05.2010